Rojava Journal of Science and Technology

2026, VOL. 3, No 1, [159-167]

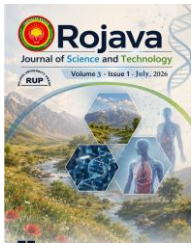

Effect of Methanol Vapor on an MQ2-MQ7-MQ9-MQ135 Metal-Oxide Gas Sensor Array: Normalized Response Fingerprints, Dynamic Behavior, and Electronic-Nose Front-End Implications

Khalil Ali Al-Ali [(1)]; Mahmood Mohammed Kareem [(2)]

1- Department of Physics, Institute of Science and Modern Technology, University of Rojava, Syria.

2- Kifri Technical College, Garmian Polytechnic University, Kurdistan Region, Iraq.

ABSTRACT

This work characterizes the methanol-vapor response of a four-channel MQ metal-oxide semiconductor gas-sensor array composed of MQ2, MQ7, MQ9, and MQ135 under controlled-flow conditions at approximately 1000 ppm. Sensor resistance was recorded once per second during methanol exposure and subsequent clean-air recovery. The extracted descriptors included baseline resistance, stabilized methanol resistance, normalized relative resistance response, response time, recovery time, response slope, exponential transient constants, and the array-level response fingerprint. All sensors showed resistance decreases under methanol, consistent with n-type SnO2-based sensors exposed to a reducing volatile compound. Under the present experimental conditions, MQ135 produced the largest normalized response (98.47%) and the strongest absolute slope (1.623 kΩ/s), MQ7 showed a similarly large normalized response (96.15%), MQ2 exhibited the shortest operational response time (25 s), and MQ9 exhibited the shortest operational recovery time (150 s). The combined amplitude-kinetic pattern provides a multidimensional feature space that may serve as a low-cost sensing front end for subsequent electronic-nose development. The present study is a sensor-array characterization at a single nominal methanol concentration; multi-concentration calibration, controlled humidity perturbation, independent-day reproducibility testing, and validated pattern-classification studies are required before broader analytical recognition claims can be made.

ARTICLE HISTORY

Received: 14 Oct. 2025

Revised: 10 May. 2026

Accepted: 28 Sep. 2026

Keywords: MQ sensors; methanol vapor; metal oxide; gas-sensor array; normalized resistance response; electronic-nose front end; fingerprint.

*Corresponding author: **Mahmood Mohammed Kareem, mahmood.mohammed@garmian.edu.krd**

1. Introduction

MQ-family metal-oxide semiconductor (MOS) sensors are widely used for low-cost volatile-organic-compound monitoring because they are compact, inexpensive, and compatible with simple resistance-readout circuits. Their analytical value increases when response amplitude is evaluated together with response time, recovery time, stability, and repeatability [1,2,3]. Methanol is a toxic volatile alcohol encountered in laboratories, fuel-related applications, fermentation monitoring, indoor air-quality assessment, and occupational-safety control. In n-type SnO2-based MOS sensors, reducing methanol molecules react with adsorbed oxygen species and return electrons to the conduction path, producing a measurable resistance decrease [1,2]. A single MQ sensor is typically cross-sensitive to several reducing gases, whereas a multichannel array can generate a response pattern that contains complementary analyte-dependent information. This work evaluates the methanol response of an MQ2-MQ7-MQ9-MQ135 array at approximately 1000 ppm and focuses on descriptors potentially suitable for subsequent electronic-nose development: normalized relative resistance response, response time, recovery time, slope, resistance contrast, and normalized multivariate fingerprints [4,5,6]. The objective is sensor-array characterization and feature extraction rather than validation of a complete automated classifier.

2. Materials and Methods

2.1. Designed System

The measurement platform consisted of a vapor-generation chamber, a controlled vapor/air delivery path, a sensor chamber containing the MQ2, MQ7, MQ9, and MQ135 sensors, flow-control elements, temperature and relative-humidity monitoring, load-resistance conditioning circuits, and a data-acquisition interface. The platform and measurement protocol were adapted from the locally designed MQ-sensor characterization system [7].

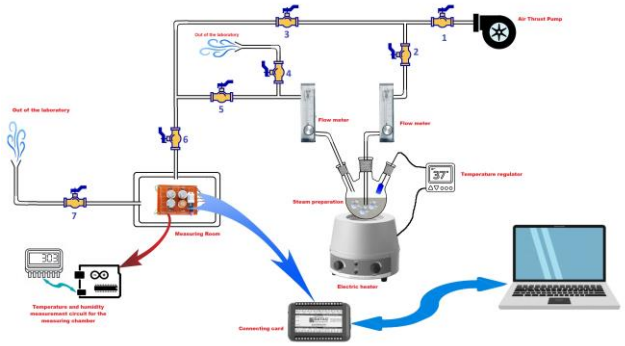

Schematic diagram of the designed measurement system, showing the vapor-exposure path, clean-air reactivation path, and electrical/data-acquisition path.

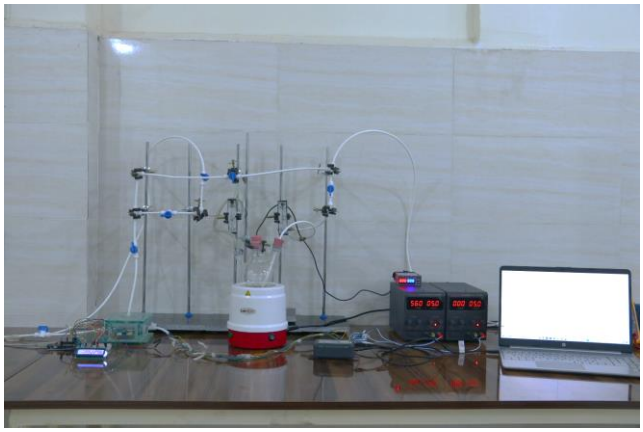

Figure 1: Experimental characterization platform for vapor delivery, sensor-chamber exposure, and data acquisition.

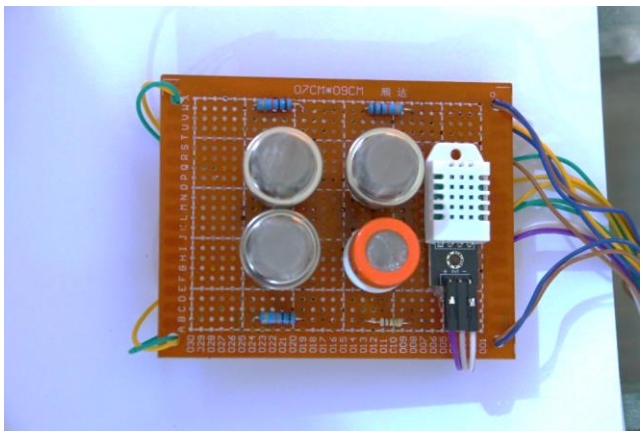

Figure 2: Sensor-board arrangement and chamber monitoring used for the MQ sensor array.

2.2. Vapor generation and flow-control mechanism

Methanol vapor at approximately 1000 ppm was introduced through the controlled vapor path for 15 min, followed by clean-air purge for 15 min to recover the sensors. Before

each measurement day, air was passed through the sensor chamber for approximately 2 h to stabilize the baseline. The voltage across the load resistance was recorded once per second and converted to sensor resistance. The operating voltage, chamber conditions, and flow arrangement were kept fixed during comparative measurements. Temperature and relative humidity were monitored as experimental control variables; they were not intentionally varied as independent factors in the present study.

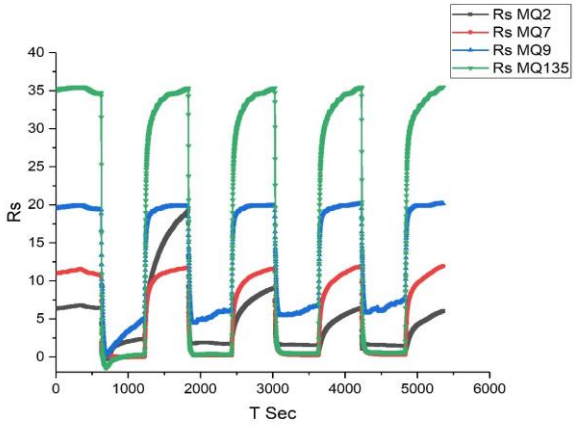

Figure 3: Repeated within-day response/recovery cycles of the MQ2-MQ7-MQ9-MQ135 array under methanol exposure and clean-air recovery.

2.3. Sensor set, operating conditions, and extracted descriptors

The tested array consisted of MQ135, MQ9, MQ7, and MQ2 sensors operated with a 5 V heater voltage and fixed load-resistance readout. According to the manufacturer manuals, these commercial MQ sensors use SnO2-based sensing layers and simple load-resistance circuits [8,9,10,11]. For each sensor, the initial air resistance R0 and the stabilized resistance during methanol exposure Rs were extracted from the resistance-time curve. Because all sensors showed a resistance decrease under methanol, the dimensionless parameter S was calculated as the normalized relative resistance response defined below. In this manuscript, S is retained as the response symbol for continuity with the experimental dataset; at a single concentration it should not be interpreted as concentration sensitivity in the calibration-curve sense. The response time ts was defined operationally as the elapsed time from vapor introduction to the stable methanol-response criterion applied consistently to all channels, while the recovery time tr was defined analogously during clean-air purge. These values are operational kinetic descriptors rather than standardized t90 metrics. The transient response and recovery curves were fitted with first-order exponential functions, and the corresponding fitted time constants were retained as kinetic descriptors. The slope was used as a practical response-rate index.

$$S = \frac{R_0 - R_s}{R_0} \times 100\%$$

The response and clean-air recovery transients were represented by the following first-order exponential models, where $b_{response}$ and $b_{recovery}$ are the fitted time constants in seconds:

$$R_{response}(t) = R_s + (R_0 - R_s)\, exp(-t/b_{response}) \quad (1)$$

$$R_{recovery}(t) = R_0 - (R_0 - R_s)\, exp(-t/b_{recovery}) \quad (2)$$

3. Results and Discussion

3.1. Resistance transients and repeatability

Before discussing the transient curves, the extracted numerical descriptors are summarized in Table 1. These values describe the analyzed exposure curves and provide the basis for the normalized-response comparison, kinetic analysis, and exponential-fit interpretation presented below. Formal between-day statistical bounds are not inferred from these single-condition descriptors.

Table 1:Extracted methanol-response descriptors for the MQ2-MQ7-MQ9-MQ135 array at approximately 1000 ppm methanol vapor.

Sensor	R0 (kΩ)	Rs (kΩ)	R0/Rs	S (%)	ts (s)	tr (s)	Slope (kΩ/s)	b_resp (s)	b_rec (s)
MQ135	34.73	0.53	65.53	98.47	30	180	-1.623	7.74	25.76
MQ9	19.86	5.47	3.63	72.46	35	150	-0.430	15.3	15.21
MQ7	11.44	0.44	26.00	96.15	40	215	-0.465	11.87	60.3
MQ2	9.17	1.74	5.27	81.00	25	230	-0.307	6.41	184.45

Note: S is the normalized relative resistance response defined in Section 2.3 at the tested nominal concentration; it is not a concentration-response calibration slope.

The resistance-time curves showed qualitatively consistent repeated within-day methanol response cycles across the array. In all four sensors, methanol exposure caused a resistance decrease, followed by resistance recovery when air was reintroduced. This behavior confirms that the selected MQ sensors responded to methanol as a reducing vapor under the present heater and flow conditions. The individual transient curves were represented by first-order exponential functions, supporting the use of fitted kinetic constants as additional descriptive features. Because formal independent-day statistics were not available in the present dataset, Figure 3 should be interpreted as evidence of within-day repeatability rather than inter-day reproducibility.

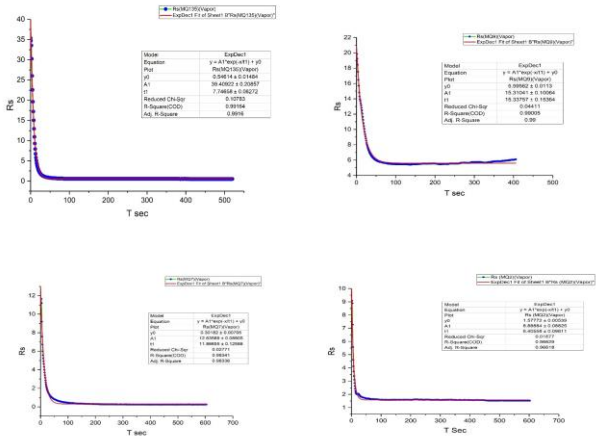

Figure 4: Exponential fits of the methanol-response transients for MQ135, MQ9, MQ7, and MQ2.

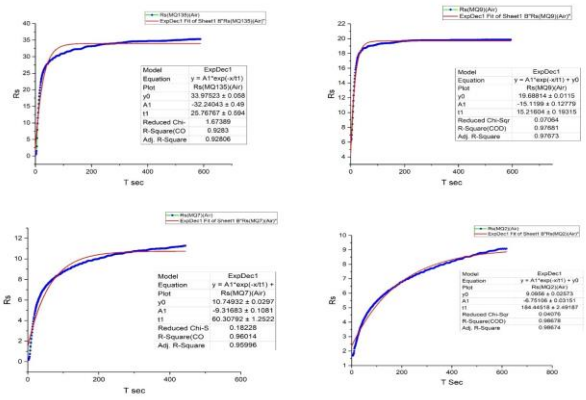

Figure 5: Exponential fits of the air-recovery transients after methanol exposure for MQ135, MQ9, MQ7, and MQ2.

3.2. Normalized response and resistance-contrast ranking

The normalized methanol-response ranking was MQ135 > MQ7 > MQ2 > MQ9. MQ135 reached S = 98.47%, corresponding to a very large resistance change from 34.73 kΩ in air to 0.53 kΩ under methanol. MQ7 also produced a strong normalized response of 96.15%, with a resistance decrease from 11.44 kΩ to 0.44 kΩ. MQ2 showed an intermediate response of 81.00%, while MQ9 showed the smallest response of 72.46%. The resistance-contrast index R0/Rs gives a similar interpretation: MQ135 and MQ7 produced the largest contrast, whereas MQ9 produced the smallest. These values describe the relative response at the tested concentration and do not represent slopes of concentration-response calibration curves.

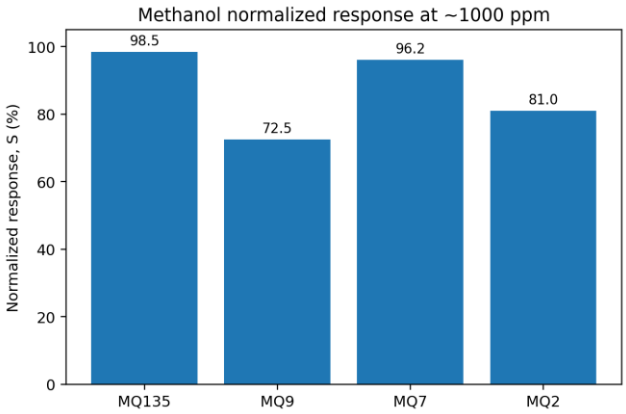

Figure 6: Normalized methanol-response ranking of the four MQ sensors (S as defined in Section 2.3).

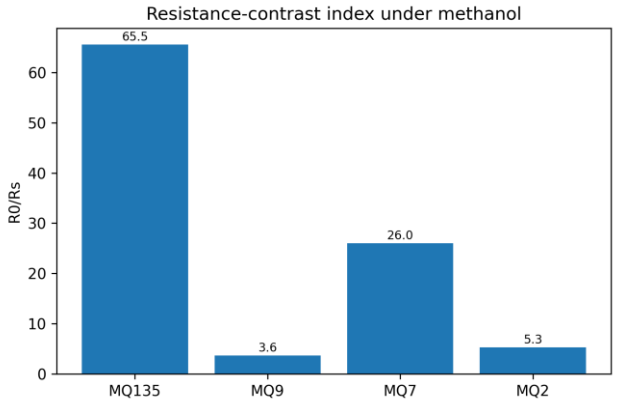

Figure 7: Resistance-contrast index R0/Rs under methanol exposure.

3.3. Response and recovery kinetics

The response times were short compared with the recovery times. MQ2 was the fastest responding channel with ts = 25 s, followed by MQ135 at 30 s, MQ9 at 35 s, and MQ7 at 40 s. Recovery required longer times for all sensors: 150 s for MQ9, 180 s for MQ135, 215 s for MQ7, and 230 s for MQ2. This asymmetry between response and recovery is consistent with MOS-sensor operation, where surface reaction during vapor exposure can be faster than desorption and surface re-oxidation during the air purge.

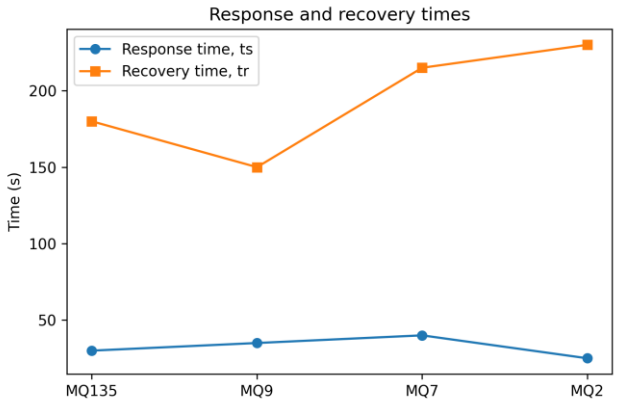

Figure 8: Response and recovery times of the MQ2-MQ7-MQ9-MQ135 array under methanol exposure.

The measured slope provided an additional kinetic separation among sensors. MQ135 had the largest magnitude slope (1.623 kΩ/s), confirming it as the dominant fast-amplitude channel. MQ7 and MQ9 had similar slope magnitudes, 0.465 and 0.430 kΩ/s, respectively, while MQ2 had the smallest slope magnitude of 0.307 kΩ/s. Therefore, MQ2 is the fastest according to response-time criterion, but MQ135 has the steepest resistance-change rate and the largest amplitude contrast.

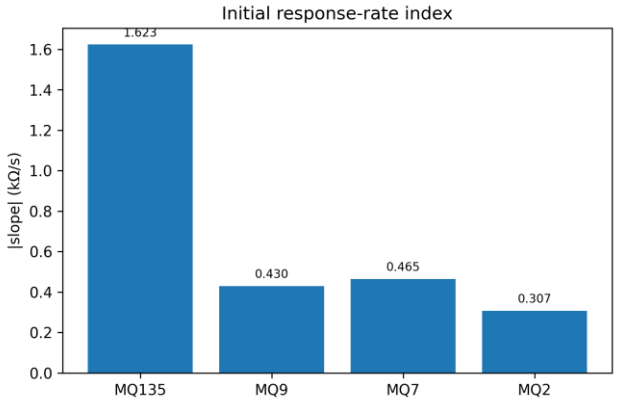

Figure 9: Absolute value of the measured response slope for each methanol-exposed sensor.

3.4. Methanol fingerprint of the MQ array

The methanol fingerprint can be represented as a multidimensional feature vector rather than by a single response value. Its prominent components are the large MQ135 and MQ7 normalized responses, the short MQ2 operational response time, the short MQ9 operational recovery time, and the dominant MQ135 slope

magnitude. This combination of amplitude, speed, recovery, and transient-shape descriptors provides a candidate feature space for subsequent electronic-nose pattern-recognition studies; it does not, by itself, demonstrate classification performance.

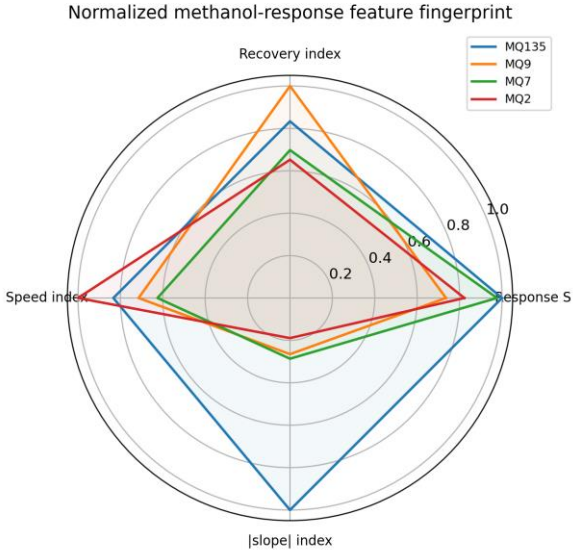

Figure 10: Normalized multidimensional methanol feature fingerprint combining response amplitude, response rate, response speed, and recovery speed.

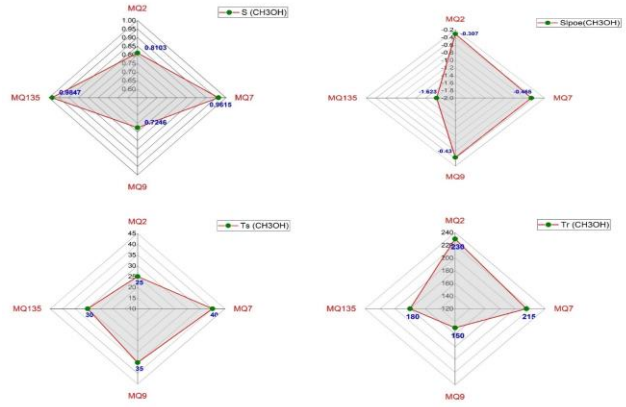

Figure 11: Methanol feature-fingerprint plots for normalized response, slope, operational response time, and operational recovery time.

3.5. Practical interpretation and cross-vapor comparison

The observed resistance decreases agree with the accepted mechanism of n-type MOS sensors under reducing gases. In air, adsorbed oxygen species remove electrons from the SnO2 surface and form an electron-depletion region, increasing resistance. Methanol molecules react with these oxygen species on the heated surface, releasing electrons and decreasing resistance. Although the four sensors share this general mechanism, the different response amplitudes and kinetics indicate that their sensing-layer composition, catalyst formulation, and heater-coupled operating state differ sufficiently to produce an analyte-specific pattern. The largest methanol-response amplitudes in this array were observed for MQ135 and MQ7. MQ135 provided the largest normalized response, the largest resistance contrast, and the steepest slope under the present conditions. MQ7 supplied a nearly comparable normalized response but with a longer operational response time than MQ135. MQ2 was not the strongest amplitude channel, but it showed the shortest operational response time, providing a distinct kinetic contribution. MQ9 showed the smallest methanol response among the four channels but the shortest operational recovery time, providing an additional recovery-dynamics component to the multidimensional feature vector. The cross-vapor comparison illustrates the motivation for an array approach. The comparative normalized-response values for ethanol, methanol, and ammonia are summarized in Table 2. Methanol produced large responses in MQ135 and MQ7 but a smaller response in MQ9. Ethanol produced a different amplitude pattern in which MQ9 was stronger and MQ2 was weaker, while ammonia produced very large responses across all four sensors. These descriptive differences support the use of multichannel feature vectors in future discrimination studies. However, Table 2 alone does not establish analyte-identification accuracy, because no independently validated classifier was applied in the present work.

Table 2: Descriptive normalized-response fingerprint of the same MQ2-MQ7-MQ9-MQ135 array toward ethanol, methanol, and ammonia.

Sensor	Ethanol S (%)	Methanol S (%)	Ammonia S (%)
MQ135	96.60	98.47	99.91
MQ9	83.10	72.46	99.93
MQ7	89.25	96.15	98.57
MQ2	60.82	81.00	99.00

Note: The cross-vapor values are descriptive response amplitudes from the same sensor-array framework and are not, by themselves, evidence of validated classification accuracy.

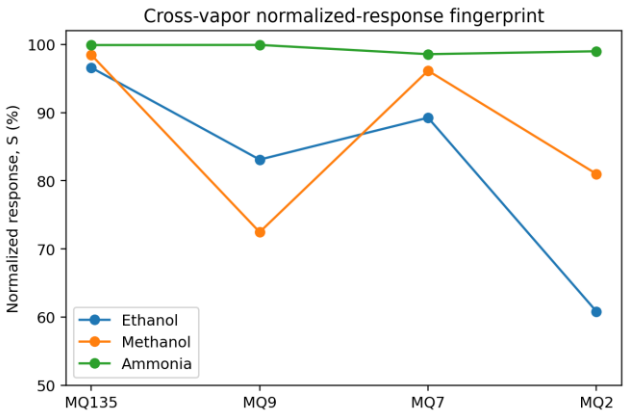

Figure 12: Descriptive comparison of normalized-response fingerprints for ethanol, methanol, and ammonia across the same MQ array.

For a subsequent, fully validated electronic-nose study, these descriptors may be used as input features for principal component analysis, linear discriminant analysis, support-vector machines, random forests, or neural-network models. Such analyses should be performed on sufficiently large sets of independent exposure cycles, with appropriate separation of training and validation data to avoid temporal or replicate-level data leakage. Future datasets should also include multiple methanol concentrations, independent test days, controlled humidity perturbations, mixed-vapor cases, and formal statistical repeatability and reproducibility metrics such as standard deviation, coefficient of variation, and confidence intervals.

3.6. Study scope and limitations

The present findings are restricted to the experimental conditions investigated, particularly the approximately 1000 ppm methanol exposure used for the reported characterization. Because only a single nominal methanol concentration is analyzed here, the study does not establish a concentration-response calibration curve, analytical concentration sensitivity, limit of detection, limit of quantification, linear dynamic range, or saturation threshold. Temperature and relative humidity were monitored as control variables but were not intentionally swept; therefore, humidity-independent performance is not claimed. The repeated cycles shown in Figure 3 support qualitative within-day repeatability, whereas independent-day reproducibility requires dedicated measurements on separate days with formal statistical bounds. Finally, the cross-vapor fingerprints are descriptive: no PCA, LDA, SVM, Random Forest, neural network, or other classifier was trained and independently validated in this study. These limitations define the next experimental stage rather than diminish the value of the present array-characterization dataset.

4. Conclusions

At approximately 1000 ppm methanol vapor, the MQ2-MQ7-MQ9-MQ135 array exhibited qualitatively consistent within-day resistance decreases and distinct amplitude-kinetic response patterns. MQ135 produced the largest normalized response (98.47%), the largest resistance contrast, and the steepest slope magnitude. MQ7 also produced a large normalized response (96.15%), MQ2 showed the shortest operational response time (25 s), and MQ9 showed the shortest operational recovery time (150 s). The findings show that the methanol response of the array is more completely represented by a multichannel feature vector combining normalized response amplitude, slope, operational response time, operational recovery time, and exponential transient constants than by a single amplitude value. This multidimensional representation is suitable for subsequent pattern-recognition research, but the present

study does not claim independently validated automated methanol identification.

The four-sensor MQ array therefore provides a practical, low-cost experimental basis for methanol-response characterization and future electronic-nose front-end development under controlled conditions. Extension to multiple concentrations, controlled temperature/humidity perturbations, independent-day replication, mixed-vapor testing, and statistically validated classification is required before the system can be evaluated as a general analytical recognition platform.

Reference

1. N. Barsan, D. Koziej, and U. Weimar, "Metal oxide-based gas sensor research: How to?", Sensors and Actuators B: Chemical, 121(1), 18-35, 2007. DOI: 10.1016/j.snb.2006.09.047.
2. A. Dey, "Semiconductor metal oxide gas sensors: A review", Materials Science and Engineering B, 229, 206-217, 2018. DOI: 10.1016/j.mseb.2017.12.036.
3. G. F. Fine, L. M. Cavanagh, A. Afonja, and R. Binions, "Metal oxide semi-conductor gas sensors in environmental monitoring", Sensors, 10(6), 5469-5502, 2010. DOI: 10.3390/s100605469.
4. A. D. Wilson and M. Baietto, "Applications and advances in electronic-nose technologies", Sensors, 9(7), 5099-5148, 2009. DOI: 10.3390/s90705099.
5. J. W. Gardner and P. N. Bartlett, "A brief history of electronic noses", Sensors and Actuators B: Chemical, 18-19, 211-220, 1994. DOI: 10.1016/0925-4005(94)87085-3.
6. Z. Zhang, Z. Zheng, X. He, K. Liu, M. Debliquy, Y. Zhou, and C. Zhang, "Electronic nose based on metal oxide semiconductor sensors for medical diagnosis", Progress in Natural Science: Materials International, 34(1), 74-88, 2024. DOI: 10.1016/j.pnsc.2024.01.018.
7. K. A. Al-Ali, Design of a System to Study the Sensitivity and Characterization for a Group of MQ Gas Sensors and Specify their Parameters for Ethanol, Methanol and Ammonia Vapors, PhD Thesis, University of Rojava, Qamishlo, Syria, 2025.
8. Zhengzhou Winsen Electronics Technology Co., Ltd., MQ-2 Semiconductor Sensor for Flammable Gas, Manual, Ver. 1.4.2024.
9. Zhengzhou Winsen Electronics Technology Co., Ltd., MQ-7 Semiconductor Sensor for Carbon Monoxide, Manual, Ver. 1.3. 2014.
10. Zhengzhou Winsen Electronics Technology Co., Ltd., MQ-9B Semiconductor Sensor for Carbon Monoxide and Methane, Manual.2021.
11. Zhengzhou Winsen Electronics Technology Co., Ltd., MQ135 Semiconductor Sensor for Air Quality, Manual, Ver. 1.4.2021.